Supercooled Smectic Nanoparticles: A Potential Novel Carrier System for Poorly Water Soluble Drugs

J. Kuntsche,[1] K. Westesen,[1,†] M. Drechsler,[1,2] M. H. J. Koch,[3] and H. Bunjes[1,4]

Received March 19, 2004; accepted June 6, 2004

Purpose. The possibility of preparing nanoparticles in the supercooled thermotropic liquid crystalline state from cholesterol esters with saturated acyl chains as well as the incorporation of model drugs into the dispersions was investigated using cholesteryl myristate (CM) as a model cholesterol ester.

Methods. Nanoparticles were prepared by high-pressure melt homogenization or solvent evaporation using phospholipids, phospholipid/bile salt, or polyvinyl alcohol as emulsifiers. The physicochemical state and phase behavior of the particles was characterized by particle size measurements (photon correlation spectroscopy, laser diffraction with polarization intensity differential scattering), differential scanning calorimetry, X-ray diffraction, and electron and polarizing light microscopy. The viscosity of the isotropic and liquid crystalline phases of CM in the bulk was investigated in dependence on temperature and shear rate by rotational viscometry.

Results. CM nanoparticles can be obtained in the smectic phase and retained in this state for at least 12 months when stored at 23°C in optimized systems. The recrystallization tendency of CM in the dispersions strongly depends on the stabilizer system and the particle size. Stable drug-loaded smectic nanoparticles were obtained after incorporation of 10% (related to CM) ibuprofen, miconazole, etomidate, and 1% progesterone.

Conclusions. Due to their liquid crystalline state, colloidal smectic nanoparticles offer interesting possibilities as carrier system for lipophilic drugs. CM nanoparticles are suitable model systems for studying the crystallization behavior and investigating the influence of various parameters for the development of smectic nanoparticles resistant against recrystallization upon storage.

KEY WORDS: cholesterol ester; colloidal drug carrier; colloidal emulsion; lipid nanoparticles; smectic phase.

INTRODUCTION

Drugs and other biologically active agents are often highly lipophilic and insufficiently soluble in aqueous media. Administration of such materials frequently requires the use of a solvent mixture or a carrier system to ensure adequate bioavailability or facilitate parenteral administration. Colloidal drug carrier systems are nanoparticulate vehicles in an aqueous system such as lipid emulsions, liposomes, nanoparticles, and the like (1–4). These carrier systems with particle sizes in the submicrometer range are suitable for parenteral, including intravenous administration. Colloidal fat emulsions are widely used for parenteral nutrition (5) and can also be used for the solubilization of lipophilic drugs (1). Several emulsion formulations are commercially available and in clinical use, for example, for propofol, diazepam, and etomidate. The potential for using such emulsions for sustained drug release applications and drug targeting, is, however, limited as the drug is assumed to dissociate very quickly from the emulsion particles after administration (1,6). Polymeric and solid lipid nanoparticles are being investigated as potential carrier systems for sustained or controlled drug release (3,4). The advantage of solid lipid nanoparticles compared to polymers is that they can be made exclusively from physiologic compounds and prepared by melt homogenization without use of organic solvents. Their highly ordered crystalline matrix usually severely limits their drug loading capacity (7). Moreover, they may display a complex behavior after melt homogenization, including retarded crystallization, polymorphic transitions and the potential to form gels particularly at higher concentrations and under certain stabilization conditions (7–11).

With respect to drug loading capacity and retarded drug release potential, a drug carrier system offering a compromise between highly fluid emulsion droplets and the rigid crystalline matrix of solid lipid nanoparticles that would retain the physiologic advantages of lipid based dispersions would be desirable. Due to its highly viscous but fluid state the liquid crystalline smectic phase is a promising candidate for the development of such systems. As many cholesterol esters are physiologic lipid compounds which can form liquid crystalline phases in dependence on temperature (thermotropic mesogens) we were interested in their potential for the development of liquid crystalline nanoparticles.

The classification of thermotropic liquid crystalline phases distinguishes two main mesophases, the smectic and the nematic phase. The smectic phase is a layered structure, with an almost parallel arrangement of the molecules along their long axes (Fig. 1). In the nematic phase, the molecules are still aligned side by side, but not in specific layers (Fig. 1). Cholesterol esters typically form a special form of the nematic phase, the cholesteric mesophase, with individual nematic molecule layers twisted into a helical arrangement forming a pseudo-layered structure (twisted nematic, Fig. 1). The phase behavior of a wide range of cholesterol esters in the bulk phase is well characterized (12). In contrast, information on the physicochemical properties and the phase behavior of cholesterol esters, especially those with saturated fatty acid chains, in the colloidal state is rather scarce. Most information on colloidal cholesterol ester containing particles originates from studies on lipoproteins and their analogues. Human plasma low density lipoprotein (LDL) is a physiologic carrier for cholesterol with a particle size of approximately 20 nm. In a simplified view, the structure is composed of a hydrophobic core containing mainly unsaturated cholesterol esters beside a

[1] Friedrich-Schiller-University Jena, Institute of Pharmacy, Department of Pharmaceutical Technology, D-07743 Jena, Germany.
[2] University of Bayreuth, Institute of Chemistry, Department of Macromolecular Chemistry, D-95440 Bayreuth, Germany.
[3] European Molecular Biology Laboratory, Hamburg Outstation, EMBL c/o DESY, D-22603 Hamburg, Germany.
[4] To whom correspondence should be addressed. (e-mail: Heike.Bunjes@uni-jena.de)

ABBREVIATIONS: CM, cholesteryl myristate; PL, phospholipid(s); SGC, sodium glycocholate; PVA, polyvinyl alcohol; PCS, photon correlation spectroscopy; PI, polydispersity index; LD-PIDS, laser diffraction with polarization intensity differential scattering; DSC, differential scanning calorimetry.

0724-8741/04/1000-1834/0

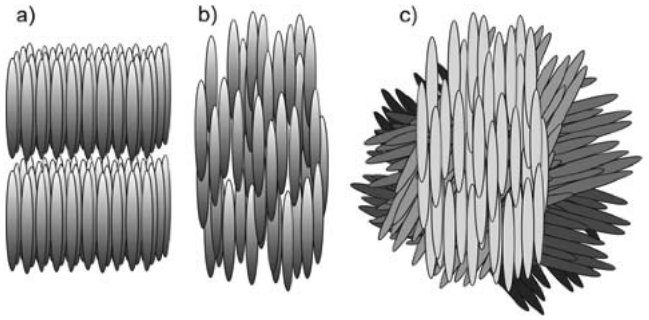

Fig. 1. Schematic presentation of the molecular order in the smectic (a), nematic (b), and cholesteric (c) mesophase.

small amount of triglycerides which is surrounded by a monolayer of phospholipids, free cholesterol and apoprotein B-100 (13). LDL-receptors are upregulated in many cancer cells that have a high demand for cholesterol due to the rapid formation of cell membranes in such neoplastic cells. Human LDL as well as LDL-like colloidal emulsions have, therefore, been investigated for an LDL-receptor targeted drug delivery (14,15). As the liquid crystalline to isotropic phase transition in human LDL and their protein free model systems is very close to or even below body temperature the ordered structure may, however, be lost under physiologic conditions (16,17). As an alternative, we have investigated the possibility of preparing nanoparticles in the thermotropic liquid crystalline state from cholesterol esters with saturated acyl chains using cholesteryl myristate as model substance.

MATERIALS AND METHODS

Materials

Materials included cholesteryl myristate (CM, Sigma, Taufen-Kirchen ICN, Eschweje), soybean phospholipids Lipoid S100 and Lipoid S75 (S100, S75, Lipoid KG, D-Ludwigshafen), sodium glycocholate (SGC, Sigma, Taufen-Kirchen), polyvinyl alcohol (PVA, Mowiol 3-83, Clariant, D-Frankfurt/Main), ibuprofen (Synopharm, D-Barsbüttel), miconazole (Abic, Il-Natanya), etomidate (Arzneimittelwerk Dresden, D-Dresden), progesterone (Jenapharm, D-Jena), thiomersal (Caesar & Loretz, D-Hilden), glycerol (Solvay, D-Rheinberg), water for injection Ph.Eur. (prepared by subsequent filtration, deionization, reverse osmosis, and distillation), cyclohexane (Ferak, D-Berlin). All materials were used as received.

Dispersion Preparation and Composition

Melt-Homogenization

The dispersions contain 5% CM (related to the whole dispersion, all concentration are w/w) as matrix lipid and different types and amounts of stabilizer system (Table I) as well as different model drugs in some systems (Table II). The CM was melted at approximately 95°C and for preparation of drug-loaded dispersions the drugs were dissolved in the cholesteryl myristate melt. SGC or PVA were dispersed in the aqueous phase containing 0.01% thiomersal and 2.25% glycerol. The phospholipids were dispersed in the aqueous phase for at least 24 h at room temperature or dissolved in the hot lipid melt. The aqueous phase containing the stabilizer(s) was heated above 90°C and added to the lipid melt. A crude emulsion was prepared by Ultra Turrax vortexing for 1–10 min at temperatures above 90°C, transferred into a heated (80–90°C) high-pressure homogenizer (Microfluidizer M110S, Microfluidics), and homogenized continuously for 5–7 min at a pressure of 650–1300 bar (Table I, Table II). After filtration through a 0.2-μm membrane (Sterifix 0.2 μm, B. Braun, Melsungen) and cooling to room temperature, the dispersions were stored at 23°C and a small fraction was stored at 4°C for comparison.

Solvent Evaporation

The dispersion was prepared by a method similar to that described by Sjöström *et al.* (18). CM (5%) and Lipoid S100 (2%) were dissolved in cyclohexane (20%). SGC (0.5%, all concentrations are related of the whole dispersion before evaporating cyclohexane) was dissolved in the aqueous phase containing 0.01% thiomersal and 2.25% glycerol. The phases were mixed and a crude emulsion was prepared by Ultra Turrax vortexing for 3–10 min at room temperature. This crude emulsion was stepwisely transferred into a high pressure homogenizer (Microfluidizer M110S, Microfluidics) and homogenized continuously for 5 min increasing the pressure from 400 to 1000 bar under ice-cooling of the interaction chamber. After combining the homogenized fractions the organic solvent was evaporated under vacuum (200 mbar) at 30–35°C in a rotary evaporator (Rotavapor 114, Büchi). The resulting dispersion was heated above 95°C for 10 min in a water bath and stored at 23°C after cooling to room temperature. For comparison, a small fraction of the dispersion was stored at 4°C.

Determination of Particle Size and Size Distribution

Photon Correlation Spectroscopy (PCS)

Dynamic light scattering at 25°C was measured at 90° with a Zeta Plus instrument (Brookhaven Instr.) after diluting the samples with purified, filtered (Sterifix 0.2 μm, Braun-Melsungen) water. The intensity weighted mean diameter (z-average diameter) and the polydispersity index (PI)—an indication for the width of the particle size distribution—were established using the instruments cumulant analysis software. The values in Table I are the average of 6–8 measurements over 5 min per run.

Laser Diffraction (LD-PIDS)

The combination of laser diffraction with the PIDS (polarization intensity differential scattering) technology (LS 230 Particle Sizer, Beckman-Coulter) allows measurements over a particle size range from about 40 nm up to 2000 μm (19). In the combined PIDS measurement the scattering of vertically and horizontally polarized light of three different wavelengths (450, 600 and 900 nm) is used and detected under different angles (60, 75, 90, 105, 120, and 146°). Data of laser diffraction and PIDS are combined to calculate the particle size distribution by the Coulter LS software (Beckmann-Coulter). Samples were measured in purified water. The values given in Table I are the average of 6–8 measurements over 90 s per run. Size distributions were calculated applying the Mie

Table I. Stabilizer Composition, Homogenization Conditions, and Particle Size of the Drug-Free Melt-Homogenized Dispersions

			Particle size[c]				
			PCS		LD-PIDS		
	Concentration of stabilizer(s)[a]	Homogenization conditions[b]	z-Average (nm)	PI	Mean (nm)	Median (nm)	D 99 (nm)
(A)	1.25% S100, 0.3 SGC	630–700 bar 5 min	174	0.13	164	141	411
(B)	2.5% S100, 0.6% SGC	650–780 bar 5 min	133	0.12	132	108	397
(C)	3.2% S100, 0.8% SGC	720–820 bar 5 min	117	0.13	115	97	370
(D)	3.2% S100, 0.8% SGC	700–1300 bar (increasing) 7 min	94	0.14	110	93	401
(E)	3.2% S100	820–840 bar 5 min	167	0.14	157	129	414
(F)	1.25% S75, 0.3% SGC	720 bar 5 min	183	0.13	178	162	418
(G)	2.5% S75, 0.8% SGC	650–750 bar 5 min	150	0.14	138	112	398
(H)	3.2% S75, 0.8% SGC	650–850 bar 5 min	137	0.13	128	105	386
(I)	3.2% S75	750 bar 5 min	177	0.11	160	137	405
(K)	1% PVA	800–900 bar 5 min	205	0.08	186	161	467
(L)	2% PVA	800–900 bar 5 min	172	0.09	145	116	420
(M)	3% PVA	900–1100 bar 5 min	148	0.11	127	101	410
(N)	4% PVA	900–1100 bar 5 min	132	0.11	120	97	409
(O)	5% PVA	900–1100 bar 5 min	124	0.12	118	96	412

[a] All dispersions contain 5% CM as matrix lipid (all concentrations refer to the whole dispersion).
[b] For the preparation of dispersions A, B, C, and E-I, variations in the compressed air supply caused fluctuations of the homogenization pressure.
[c] Particle sizes were measured within 2 days after preparation.

theory with an estimated refraction index of 1.45 and a shape factor of 1.

Differential Scanning Calorimetry

DSC measurements were made on a Pyris-1 calorimeter (Perkin-Elmer). Approximately 8–15 mg (dispersions) or 2 mg (bulk) samples were accurately weighed into standard aluminum pans. An empty pan was used as reference. The samples were heated from room temperature to 90°C (dispersions) or 95°C (bulk material) and then cooled to –8/–10°C (dispersions) or 0°C (bulk material) and heated again to 90°C or 95°C, respectively (scan rate 5°C/min). All DSC curves were normalized to a sample mass of 1 g.

The amount of recrystallized CM in the dispersions was calculated by comparing of the melting enthalpies of the first heating run (original sample) with those of the second one after cooling and crystallization of the particles (see Fig. 7). Very small amounts of crystalline material (<1% of the matrix lipid) are detectable this way. Because crystallized particles obtained by cold storage have a slightly higher melting enthalpy in the first DSC heating runs compared with heating of the freshly crystallized sample, the procedure may, slightly overestimate the crystalline content.

Electron Microscopy

Freeze-Fracture

A bare golden TEM grid (BAL-TEC, 400 mesh) was dipped into the dispersion (original emulsions) and placed between two copper specimen carriers (BAL-TEC). The sample was rapidly jet frozen with liquid propane cooled to –150°C (JFD 030, BAL-TEC) and fractured in a freeze fracture unit (BAF 060, BAL-TEC) at –150°C and 10^{-7} to 10^{-6} mbar. The fractured samples were shadowed under 45° with a 2-nm-thick platinum/carbon (Pt/C 95/5 v/v) layer and stabilized by deposition of 20 nm pure carbon under 90° for replica production. Replicas were cleaned with chloroform/methanol (50:50 v/v) and viewed with a transmission electron microscope (CEM902A, Carl Zeiss NTS GmbH) operated at 80 kV.

Table II. Composition, Homogenization Pressure, and Particle Size (Determined Directly After Preparation) of the Drug-Loaded Dispersions

Drug	Composition (related to the whole dispersion)	Homogenization conditions	Particle size[a] PCS z-Average (nm)	PCS PI	LD-PIDS Mean (nm)	LD-PIDS Median (nm)	LD-PIDS D 99 (nm)
Ibuprofen	5% CM 3.2% S100 0.8% SGC 0.5% drug	900–1200 bar 80–90°C 5 min	102	0.15	113	95	404
Miconazole	5% CM 3.2% S100 0.8% SGC 0.5% drug	1000–1300 bar 80–90°C 5 min	99	0.15	120[b]	98[b]	411[b]
Etomidate	5% CM 3.2% S100 0.8% SGC 0.5% drug	1000–1300 bar 80–85°C 5 min	94	0.16	112	93	401
Progesterone	5% CM 3.2% S100 0.8% SGC 0.05% drug	1000–1300 bar 80–90°C 5 min	99	0.14	115	95	401

[a] Particle sizes were measured directly after preparation.
[b] Results of the measurement 12 months after preparation, as no stable measurements were obtained after preparation.

Cryopreparation

A few microliters of diluted emulsion were placed on a bare copper TEM grid (Plano, 600 mesh) and the excess of liquid was removed with filter paper. This sample was cryofixed by rapid immersing into liquid ethane cooled to –170 to –180°C in a cryobox (Carl Zeiss NTS GmbH). Excess ethane was removed by blotting in the cold. The sample was transferred with a cryotransfer unit (Carl Zeiss NTS GmbH) into the pre-cooled cryoelectron microscope (CEM902A, Carl Zeiss NTS GmbH) operated at 80 kV. Samples were viewed under low-dose conditions (beam current around 1mA resulting in a cumulative specimen dose of about 0.1 C/cm^2 at a primary magnification of 30,000×) at a constant temperature around –194°C.

Polarizing Light Microscopy

The drug-loaded dispersions were examined in a Leica microscope (DMRXP, D-Wetzlar) equipped with crossed polarizers and a λ-sheet.

X-ray Diffraction

Simultaneous small and wide angle synchrotron radiation X-ray diffraction patterns were recorded with two linear delay line detectors on the X33 camera of the EMBL on the storage ring DORIS of the Deutsches Elektronen Synchrotron (DESY) (20,21). The range of scattering vectors (s = 1/d, where d is the spacing) was about 0.1–0.6 nm^{-1} for the small and 1–3.5 nm^{-1} for the wide angle range. Data reduction, background subtraction and correction for detector response were done with the program SAPOKO (22). Detector channels were calibrated with crystalline tripalmitin [assuming a long spacing of 40.6 Å (23) and short spacings of 4.6 and 3.7 Å (24)]. The sample holder was thermostated using a water bath and temperature monitored with a sensor in a reference cell.

Rheology

Measurements were performed with a plate-plate rheometer CVO 50 (Bohlin). The plate diameter was 40 mm and the plate-to-plate gap 500 μm. CM was heated to 90°C and the melt transferred into the thermostatized rheometer. Temperature dependent measurements were made at a constant shear rate of 20 s^{-1} from 90 to 60°C and a cooling rate of 0.1°C/min. Shear rate dependent measurements (between 10 s^{-1} and 160 s^{-1}) were made at 88°C for the isotropic, at 84°C for the cholesteric and at 70°C for the smectic phase.

RESULTS

Characterization of the Bulk Material

The results obtained on the bulk CM are in good agreement with the literature (12,25–27). The liquid crystalline phase transitions are each associated with small but distinct thermal transitions in DSC heating and cooling runs (Fig. 2). CM melts around 72°C forming a smectic phase transforming into the cholesteric phase around 79°C before the ester melts into an isotropic liquid around 84°C. Upon cooling of the isotropic melt, the liquid crystalline phase transitions are observed at about the same temperatures as observed upon heating, whereas the smectic phase displays high supercooling with crystallization occurring only around 40°C. (The term supercooling refers to the temperature difference between melting and the subsequent crystallization upon cooling). Thermally untreated CM melts at slightly higher temperature with a slightly higher enthalpy change than the freshly crys-

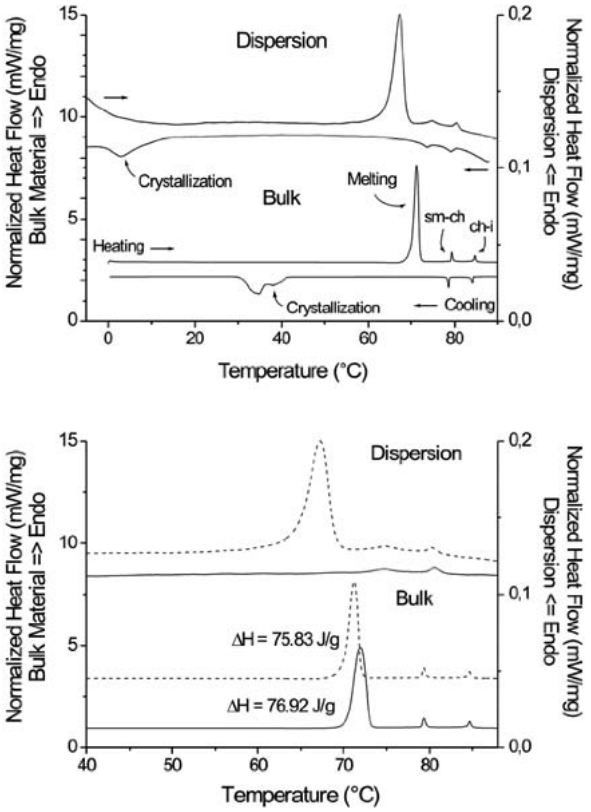

Fig. 2. Top: DSC heating and cooling curves (5°C/min) of CM in bulk and in the colloidal state (dispersion L: 2% PVA, 2 days after preparation). The samples were heated to the isotropic melt (curves not shown), cooled down below the crystallization temperature and heated again (sm-ch, smectic-cholesteric; ch-i, cholesteric-isotropic phase transition). Bottom: DSC curves of the first (thermally untreated, full line) and second (after crystallization, dashed line) heating run (5°C/min) of CM in bulk and in the colloidal state (dispersion L: 2% PVA, 2 days after preparation).

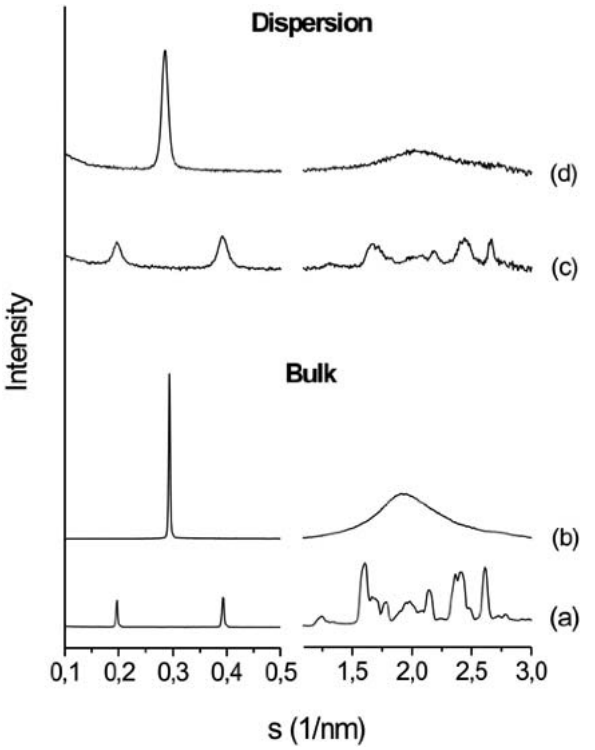

Fig. 3. Small and wide angle X-ray diffraction patterns of CM in bulk (bottom) and in colloidal dispersion (top). Bulk: crystalline powder (a) at 20°C and smectic mesophase (b) at 60°C (formed upon cooling after heating into the isotropic melt). Dispersions stored at 4°C (c) and at 23°C (d) measured at 20°C (dispersion O, 5% PVA). The graphs of the bulk material and the dispersions are not on the same (linear) intensity scale.

tallized substance (Fig. 2), presumably due to the formation of an imperfect crystal lattice upon crystallization at this comparatively high cooling rate (5°C/min). It should be borne in mind that the crystallization temperature depends on the cooling rate and increases at lower scan rate.

Due to its layered structure the smectic phase gives a sharp intense small angle X-ray reflection at a spacing of about 34.1 Å at 60°C (Fig. 3), which decreases with increasing temperature due to a stronger interpenetration of the molecules in adjacent layers (26). In the temperature range of the cholesteric phase only a very broad and weak small angle X-ray reflection was observed. In the wide angle range, there is only diffuse scattering for both liquid crystalline phases because of molecular disorder compared to the crystalline phase. Crystalline CM gives a characteristic diffraction pattern with a long spacing of about 50.6 Å (first order) at 20°C (Fig. 3).

The viscosity of CM strongly depends on temperature and the liquid crystalline phase transitions are reflected in clear alterations of the rheological behavior in temperature dependent measurements (Fig. 4). With decreasing temperature, the viscosity of the smectic phase increases nearly linearly to about 5 Pa·s at 60°C at a shear rate of 20 s^{-1}. The viscosity of the cholesteric and the isotropic phase is much lower than that of the smectic phase. Whereas the isotropic phase displays a nearly Newtonian flow, the viscosity of both the smectic (Fig. 4) and the cholesteric phase decreases with increasing shear rate. The cholesteric phase is much more sensitive against shear stress as indicated by rapid decrease of viscosity already at low shear rate. Moreover, the rheogram of the cholesteric phase displays a larger hysteresis than that of the smectic phase indicating a slower reorganization of the cholesteric structure (data not shown).

Characterization of Drug-Free Dispersions

Macroscopic Appearance and Particle Size

High-pressure melt homogenization leads to fine, white to slightly yellowish dispersions with PCS z-average diameters between about 95 and 210 nm and PI between 0.08 and 0.14 (Table I). With increasing stabilizer concentrations, the particle size decreases (Fig. 5). Phospholipid/bile salt combinations are more efficient for the preparation of small particles than stabilization only by phospholipids. The highly purified soybean lecithin S100, which contains at least 94% phosphatidylcholine, gives slightly smaller particles than S75, which contains besides phosphatidylcholine (68–73%) up to 10% phosphatidylethanolamine (all concentrations are manufacturer's specifications) and other minor components. Although the PVA stabilized dispersions were prepared at higher pressure, the dispersions have larger particles (Fig. 5). The par-

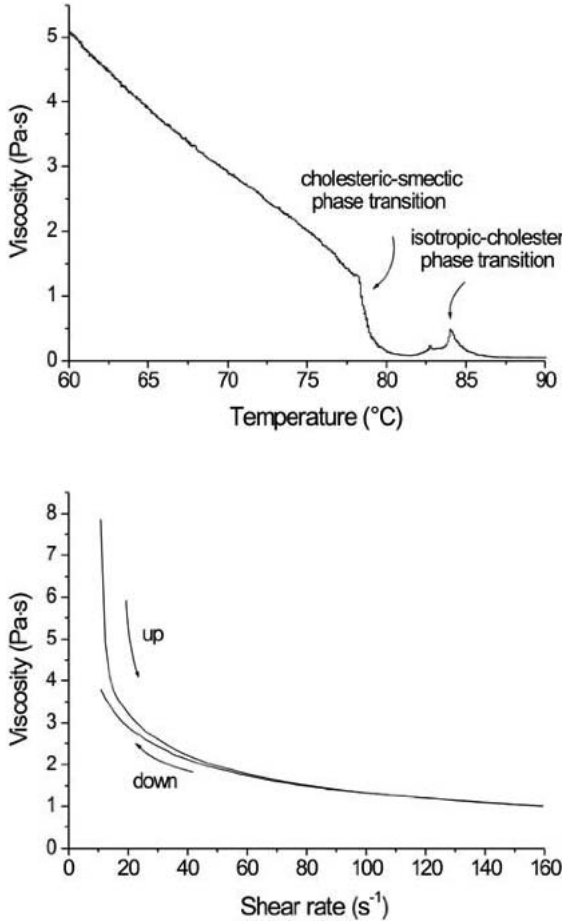

Fig. 4. Viscosity of CM as a function of temperature (cooling at 0.1°C/min) at a shear rate of 20 s^{-1} (top) and of shear rate at 70°C (bottom).

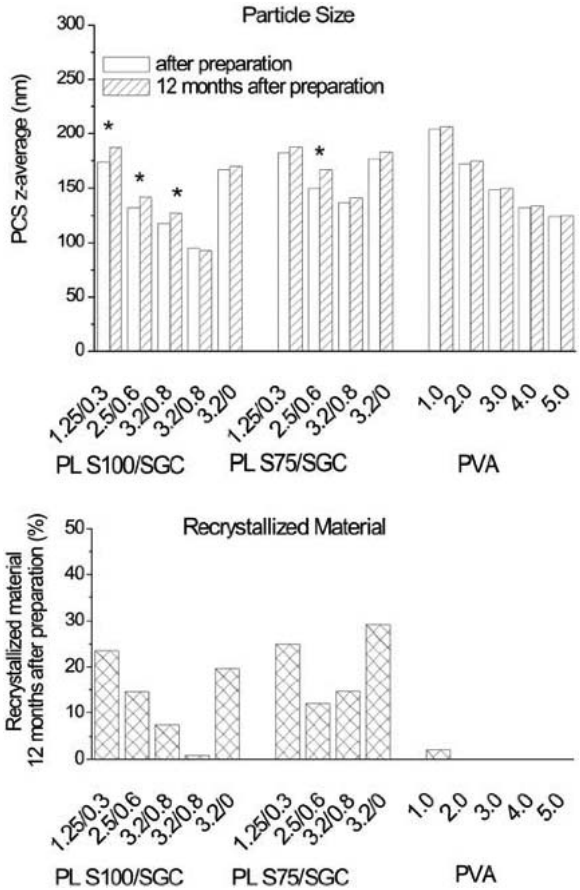

Fig. 5. Particle size after preparation (determined within to 2 days) and after 12 months storage (top) and amount of recrystallized matrix lipid after storage (bottom). Dispersions with a particle size increase above 5% are marked with an asterisk.

ticle size distributions by volume (LD-PIDS) are bimodal with maxima at approximately 100 nm and 300–350 nm for all dispersions (Fig. 6). Even though a direct comparison of the results of the different particle sizing methods is not possible, the results of the PCS- and LD-PIDS-measurements are in good agreement.

Twelve months after preparation all dispersions still appear homogenous, except for a very small sediment, especially in dispersions with larger particle sizes, which can easily be redispersed by gentle shaking. The PCS z-average diameters are at most 5% larger after storage except for four dispersions (Fig. 5). This particle growth was generally not so clear in the LD-PIDS measurements and more pronounced in dispersions stabilized with phospholipids.

For all dispersions the fractions stored at 4°C (in which the CM particles are in the crystalline state) had a slightly larger z-average than those stored at 23°C [e.g., 1 month after preparation the value for the dispersion stabilized with 3.2% S100 and 0.8% SGC (dispersion C) was 127 nm for the crystalline (stored at 4°C) and 116 nm for the smectic (stored at 23°C) nanoparticles]. Electron micrographs of dispersions stored at 4°C indicate an anisometric platelet-like structure of crystalline CM particles (data not shown), which could explain the higher z-averages in PCS-measurements (8,28).

With the solvent evaporation method, a dispersion with very small particles was obtained. The PCS z-average of the fine, translucent, slightly yellow dispersion was 38 nm with a PI of 0.11 and did not increase during 12 months of storage.

Phase Behavior

On DSC analysis, the nanoparticles display essentially the same phase transitions as the bulk material albeit somewhat broadened and slightly shifted to lower temperatures,

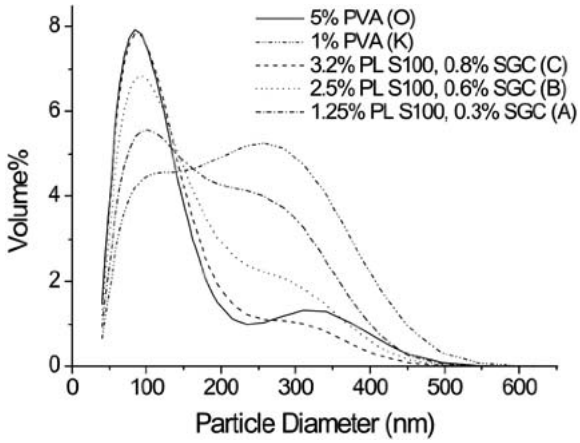

Fig. 6. Particle size distribution (LD-PIDS) of selected dispersions measured after preparation (within to 2 days).

except for the smectic-to-crystalline transition where supercooling is significantly higher than in the bulk material (Fig. 2). Crystallization occurs only below room temperature in the dispersions with storage at 4°C leading to crystallization of the nanoparticles.

The recrystallization tendency upon storage at room temperature strongly depends on the stabilizer system and the particle size. Only the dispersion with the lowest PVA content (1% PVA) contained a very small amount of recrystallized material 12 months after preparation (Fig. 5), despite the relatively high PCS z-averages of the PVA-based dispersions. In contrast, the recrystallization tendency of the phospholipid based systems is much higher and increases with particle size. Only in the dispersions with very small particles (the one prepared by solvent evaporation and the melt-homogenized dispersion D with 3.2% S100 and 0.8% SGC) was no or only a very small amount (below 1%) of recrystallized material observed after 12 months storage.

The large difference in the crystallization tendency between phospholipid and PVA-based dispersions may result from their different crystallization behavior observed in DSC cooling runs. Phospholipid based dispersions usually display two crystallization events (Fig. 7). With increasing particle size, the area under the crystallization peak at higher temperatures increases. In addition, the crystallization behavior changes upon storage and depends on thermal treatment (e.g., whether the dispersion was heated prior to crystallization or not). PVA stabilized CM nanoparticles usually show only one crystallization event (Fig. 7). For hitherto unknown reasons, the crystallization enthalpy is smaller than that of the phospholipids based systems and decreases with increasing amounts of polymer and upon storage.

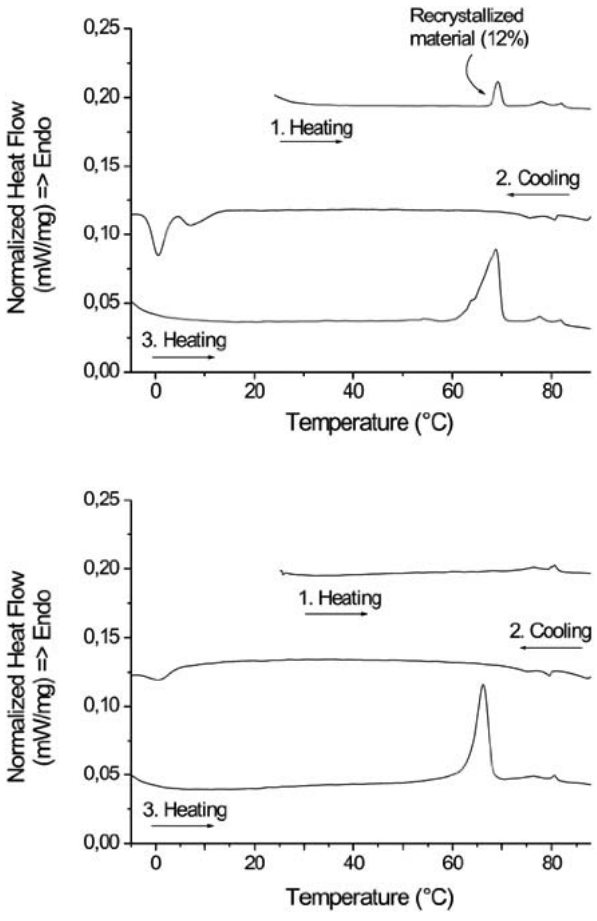

Fig. 7. DSC-heating and cooling curves (5°C/min) of dispersion G (2.5% S75, 0.6% SGC, top) and dispersion M (3% PVA, bottom) 12 months after preparation.

Physical State

Colloidal smectic particles display the characteristic small angle X-ray reflection and only diffuse scattering in the wide angle range (Fig. 3). The reflection is weaker and broader than that of the bulk material, but its position is comparable under equivalent conditions. As in the bulk material, the spacing of the smectic layers increases with decreasing temperature, e.g., from 33.5 Å at 75°C to 35.1 Å at 20°C for dispersion C (3.2% S100, 0.8% SGC); at 60°C a spacing of 34.1 Å was observed for this dispersion. For cold stored CM nanoparticles the small and wide angle diffraction pattern characteristic of crystalline CM was detected with a long spacing of about 50.8 Å (first order) at 20°C (Fig. 3).

Ultrastructure

At least three different structures can be distinguished in cryoelectron micrographs of a phospholipid stabilized dispersion (dispersion C, 3.2% S100, 0.8% SGC) (Fig. 8). Beside liposomes (appearing as ring-shaped particles), which are formed by the excess of phospholipid, rectangular and circular structures were observed. Some of these were very unstable toward the electron beam as reflected in immediate "boiling" of the particles which could therefore not be photographed in their original state (Fig. 8). Only a fraction of the particles displays such a behavior, suggesting the existence of two different types of CM particles in the dispersion. Structured round-shaped and angular particles can also be observed in micrographs of freeze-fractured specimen of the same dispersion. Some of the round particles have an onion-like structure indicating that a fraction of the nanoparticles has a spherical shape. The non-spherical particles are probably cylindrical leading to different images in the micrographs depending on their projection (Fig. 8). Beside the two types of cholesterol ester particles, very small spherical structures with a smooth surface, which probably represent the liposomal fraction, are also present in the micrographs of the freeze-fractured dispersion.

Micrographs of a PVA-based dispersion (dispersion O, 5% PVA) have a much more homogeneous appearance with round or oval shaped particles in cryopreparation and freeze fracture (Fig. 8). No unstable particles were detected in the cryopreparation. The rough background observed in freeze fracture as well as in the cryopreparation, might result from polymer dissolved in the aqueous phase.

Drug-Loaded Dispersions

Ibuprofen, miconazole, etomidate, and progesterone were used as poorly water soluble model drugs for the preparation of drug-loaded supercooled smectic nanoparticles stabilized with S100/SGC. The lower melting drugs (melting point <90°C) ibuprofen, etomidate, and miconazole could easily be incorporated into the dispersions at an amount of 10% (w/w CM) by melting the drug together with the lipid. Progesterone, which melts at higher temperature (> 120°C), was incorporated only at 1% as the higher concentrations

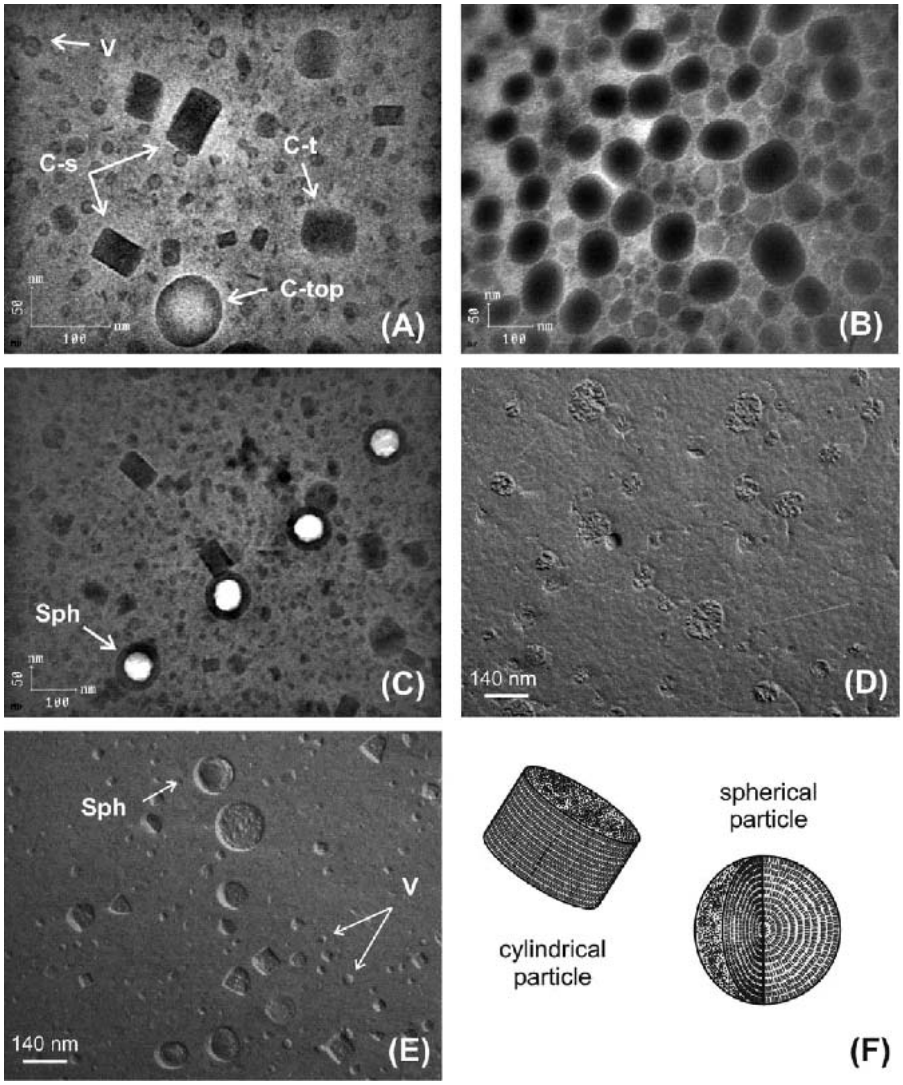

Fig. 8. Electron micrographs of dispersion C (3.2% S100, 0.8% SGC, A, C and E) and dispersion O (5.0% PVA, B and D) in cryopreparation (A–C) and freeze-fracture (D–E). A hypothetical model of the molecular order in cylindrical and spherical smectic CM nanoparticles is shown in F. C-s, cylindrical particle in side view; C-top, cylindrical particle in top view; C-t, cylindrical particle in tilted orientation; V, phospholipid vesicle; and Sph, presumably spherical particle ("boiling" in the cryopreparation).

(5%) did not dissolve in the lipid melt within appropriate time. After melt homogenization, all dispersions appear homogeneous except for a very small, slightly gray colored sediment which formed upon storage but could be easily redispersed through gentle shaking. This sediment probably is a contamination from the homogenization process. After preparation, PCS z-average values around 100 nm with polydispersity indices between 0.14 and 0.16 were found. As in the unloaded dispersions, the particle size distribution by volume (LD-PIDS) was bimodal with maxima at approximately 100 and 300 nm. No stable LD-PIDS measurements were obtained for the miconazole containing dispersion after preparation, but particle size could be measured after storage for 6 and 12 months.

The smectic state of the particles was confirmed by X-ray diffraction and DSC. Drug incorporation does not influence the spacing of the smectic layers. At 20°C spacings between 35.1 and 35.2 Å were measured in X-ray diffraction for the dispersions stored at 23°C. Incorporation of the drug molecules does, however, influence the liquid crystalline phase transition temperatures which were shifted to lower temperatures (Fig. 9).

All dispersions were stable upon storage over 12 months with respect to macroscopic appearance, particle size and particle recrystallization (Fig. 9). Only in the progesterone containing dispersion was a small amount of recrystallized material detected (4% percent after storage for 12 months). In polarizing light microscopy, no particles >5 μm and no drug precipitation were observed in the dispersions after 12 months storage at 23°C.

DISCUSSION

Smectic nanoparticles with z-average diameters between 95 and 210 nm can be prepared by high-pressure melt homog-

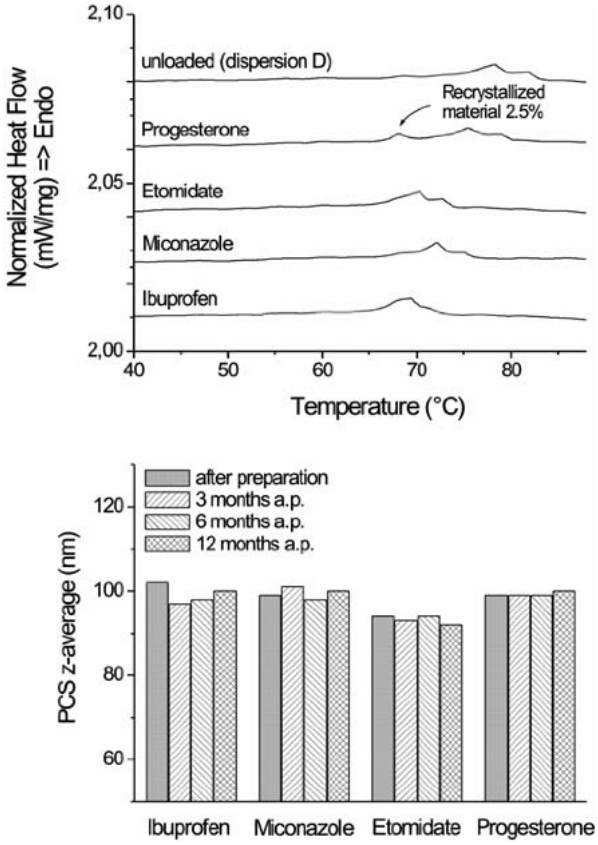

Fig. 9. Top: DSC-heating curves (5°C/min) of the original, thermally untreated dispersions measured 6 months after preparation. Bottom: Particle size (PCS) of the drug-loaded dispersions after separation and storage.

enization of CM with the aid of phospholipids, bile salt, and PVA. The solvent evaporation method leads to much smaller particles (z-average 38 nm). In the colloidal state, the smectic phase of CM shows a considerable supercooling effect; crystallization starts only below room temperature. This phenomenon allows the preparation of smectic CM nanoparticles which are stable at room temperature even though the smectic phase does not exist under these conditions in the bulk material. Storage at 4°C leads, however, to crystallization of the CM nanoparticles. Although conclusions about the colloidal state are problematic, the rheological measurements on the smectic bulk phase point to a high viscosity of the strongly supercooled smectic phase which should be advantageous for particle stability and drug release.

Snow *et al.* already described a distinct supercooling effect for submicron emulsions of different cholesterol esters but did not investigate their long-term stability (29). The increased supercooling effect in colloidal dispersions compared to the bulk material is attributed to crystallization by homogeneous nucleation in the highly dispersed state. In the bulk phase, crystallization is usually caused by the presence of a small number of particulate impurities which promote nucleation (heterogeneous nucleation), after which crystallization can spread throughout the material. In the colloidally dispersed material the heterogeneous nuclei will end up in only a few particles leaving the large majority of particles free of nucleation-promoting impurities. This makes nucleation more difficult and requires a higher degree of supercooling to form homogeneous nuclei (30). Although an effect of the stabilizer system on the crystallization behavior of the CM nanoparticles was observed, the general supercooling phenomenon is not due to the presence of the stabilizer molecules, as investigations on bulk mixtures (in the highest ratio used in the dispersions) revealed only a depression of the crystallization temperature of a few degrees (data not shown).

All dispersions were stable upon storage for 12 months with regard to particle size and macroscopic appearance. The small increase of the particle size observed for some dispersions may at least partly be related to the relatively high amount of crystalline material in these systems, although no direct correlation between the increase in PCS z-average diameter and the amount of recrystallized material was found (Fig. 5).

The stabilizer system strongly influences the crystallization behavior of the nanoparticles upon cooling and the recrystallization tendency upon storage. PVA, which is not approved for parenteral administration, seems to be more efficient in stabilizing the supercooled smectic state against recrystallization than phospholipids. It remains to be investigated, whether polymeric stabilizers which are accepted for parenteral use, for example, poloxamers, display comparable effects. In dispersions stabilized on the base of phospholipids a bimodal crystallization pattern was observed. With increasing particle sizes the area of the crystallization peak at higher temperature increases leading to a pronounced recrystallization of CM in these dispersions upon long-term storage (Fig. 5). The causes for the bimodal crystallization pattern of the nanoparticles in phospholipid containing dispersions are not yet clear. It is conceivable, that CM particles with different shapes (cylindrical and spherical), which were observed by electron microscopy in phospholipid-containing dispersions, would have a different crystallization behavior. Moreover, interactions between cholesterol esters and phospholipids have been described (31) and some of the peculiarities observed may point to interactions of the phospholipid with the CM, resulting for example in a varying composition of the nanoparticle interface or core upon storage.

Electron microscopy of the dispersions indicates that the particles have a nearly cylindrical shape in most cases. The very unstable structures observed in the cryopreparation of the phospholipid based dispersion are, however, probably spherical. Due to the layered structure of the smectic phase, a cylindrical particle shape should be energetically more favorable than a spherical one, which might be the cause for an increased sensitivity of the spherical particles toward the electron beam. Similar cylindrical structures were described in an electron microscopic study on human low density lipoproteins (LDL) (32). In this study, the samples were prepared at room temperature, so that the electron microscopy images should display the human LDL particles in their liquid crystalline state.

Smectic CM nanoparticles could be loaded with different model drugs without loss of the supercooled smectic state. The lower melting substances were incorporated in the dispersions at a concentration of 10% whereas progesterone could only be dissolved in the lipid melt with at a concentration of 1% related to the CM at appropriate dissolution times. Drug incorporation does not influence the spacing of the smectic layers, but the shift of the liquid crystalline phase transitions clearly indicates an interaction of the drug mol-

ecules with the smectic phase and thus an association with the nanoparticles matrix. The observed instability of the miconazole loaded dispersion in LD-PIDS measurements after preparation could be due to an interaction of the drug with the interfacial layer resulting in a higher sensitivity against dilution. All drug-loaded systems under investigation were stable upon storage for 12 months with respect to macroscopic appearance, particle size, drug precipitation and physicochemical state of the nanoparticles.

CONCLUSIONS

Due to the highly viscous but fluid liquid crystalline state of their matrix lipid, colloidal smectic nanoparticles offer promising possibilities as delivery systems for lipophilic drugs. Because the supercooled smectic phase is metastable, investigations on the crystallization behavior of the nanoparticles are important for developing such dispersions. Nanoparticles based on pure CM usually crystallize above 0°C, making them interesting model systems to investigate the influence of various parameters on their crystallization behavior. It may, however, be difficult to process this matrix material into drug carrier systems which are stable under usual conditions of transport, storage and handling as the crystallization tendency is still fairly high. Further efforts are thus directed at suppressing recrystallization upon storage, in particular by variation of the matrix composition. Moreover, further investigations especially on the localization of the drug molecules in the dispersions as well as drug release are required to evaluate the potential advantage of smectic nanoparticles as drug delivery system in more detail.

ACKNOWLEDGMENTS

The authors thank Steffi Richter and Jürgen Mehlem for support in the electron microscopic investigations and rheological measurements, respectively.

REFERENCES

1. S. Klang and S. Benita. Design and evaluation of submicron emulsions as colloidal drug carriers for intravenous administration. In S. Benita (ed.), *Submicron Emulsions in Drug Targeting and Delivery*, Harwood Academic Publishers, Amsterdam, 1998, pp. 119–152.
2. A. Sharma and U.S. Sharma. Liposomes in drug delivery: progress and limitations. *Int. J. Pharm.* **154**:123–140 (1997).
3. E. Fattal and C. Vauthier. Nanoparticles as drug delivery systems. In J. Swarbrick and J. C. Boylan (eds.), *Encyclopedia of Pharmaceutical Technology*, Marcel Dekker, New York, 2002, pp. 1864–1882.
4. W. Mehnert and K. Mäder. Solid lipid nanoparticles. Production, characterization and applications. *Adv. Drug. Deliver. Rev.* **47**: 165–196 (2001).
5. Y. A. Carpentier and I. E. Dupont. Advances in intravenous lipid emulsions. *World J. Surg.* **24**:1493–1497 (2000).
6. C. Washington and K. Evans. Release rate measurements of model hydrophobic solutes from submicron triglyceride emulsions. *J. Control. Rel.* **33**:383–390 (1995).
7. K. Westesen, H. Bunjes, and M. H. J. Koch. Physicochemical characterization of lipid nanoparticles and evaluation of their drug loading capacity and sustained release potential. *J. Control. Rel.* **48**:223–236 (1997).
8. H. Bunjes, K. Westesen, and M. H. J. Koch. Crystallization tendency and polymorphic transitions in triglyceride nanoparticles. *Int. J. Pharm.* **129**:159–173 (1996).
9. K. Westesen and B. Siekmann. Investigation of the gel formation of phospholipid-stabilized solid lipid nanoparticles. *Int. J. Pharm.* **151**:35–45 (1997).
10. H. Bunjes, M. H. J. Koch, and K. Westesen. Influence of emulsifiers on the crystallization of solid lipid nanoparticles. *J. Pharm. Sci.* **92**:1509–1520 (2003).
11. C. Freitas and R. H. Müller. Effect of light and temperature on zeta potential and physical stability in solid lipid nanoparticles (SLN) dispersions. *Int. J. Pharm.* **168**:221–229 (1998).
12. G. S. Ginsburg, D. Atkinson, and D. M. Small. Physical properties of cholesteryl esters. *Prog. Lipid Res.* **23**:135–167 (1984).
13. T. Hevonoja, M. O. Pentikäinen, M. T. Hyvönen, P. T. Kovanen, and M. Ala-Korpela. Structure of low density lipoprotein (LDL) particles: Basis for understanding molecular changes in modified LDL. *Biochim. Biophys. Acta* **1488**:189–210 (2000).
14. R. A. Firestone. Low-density lipoprotein as vehicle for targeting antitumor compounds to cancer cells. *Bioconj. Chem.* **5**:105–113 (1994).
15. R. C. Maranhão, S. R. Graziani, N. Yamaguchi, R. F. Melo, M. C. Latrilha, D. G. Rodrigues, R. D. Couto, S. Schreier, and A. C. Buzaid. Association of carmustine with a lipid emulsion: In vitro, in vivo and preliminary studies in cancer patients. *Cancer Chemoth. Pharmacol.* **49**:487–498 (2002).
16. K. Westesen, A. Gerke, and M. H. J. Koch. Characterization of native and drug-loaded human low density lipoproteins. *J. Pharm. Sci.* **84**:139–147 (1995).
17. A. Gerke, K. Westesen, and M. H. J. Koch. Physicochemical characterization of protein-free low density lipoprotein models and influence of drug loading. *Pharm. Res.* **13**:1–8 (1996).
18. B. Sjöström, B. Kronberg, and J. Carlfors. A method for the preparation of submicron particles of sparingly water soluble drugs by precipitation in o/w-emulsions. I. Influence of emulsification and surfactant concentration. *J. Pharm. Sci.* **82**:579–583 (1993).
19. Renliang Xu. Improvements in particle size analysis using light scattering. In R. H. Müller and W. Mehnert (eds.), *Particle and Surface Characterizing Methods.* Scientific Publisher, Stuttgart, 1997, pp. 27–56.
20. M. H. J. Koch and J. Bordas. X-ray diffraction and scattering on disordered systems using synchrotron radiation. *Nucl. Instrum. Methods* **208**:461–469 (1983).
21. G. Rapp, A. Gabriel, M. Dosière, and M. H. J. Koch. A dual detector single readout system for simultaneous small (SAXS) and wide angle X-ray (WAXS) scattering. *Nucl Instrum Methods A* **357**:178–182 (1995).
22. P. V. Konarev, V. V. Volkov, A. V. Sokolova, M. H. J. Koch, and D. I. Svergun. PRIMUS – a Windows-PC based system for small-angle scattering data analysis. *J. Appl. Crystallogr.* **36**:1277–1282 (2003).
23. D. Chapman. The polymorphism of glycerides. *Chem. Rev.* **62**: 433–456 (1962).
24. C. W. Hoerr and F. R. Paulicka. The role of X-ray diffraction in studies of the crystallography of monoacid saturated triglycerides. *J. Am. Oil Chem. Soc.* **45**:793–797 (1968).
25. G. J. Davis, R. S. Porter, and E. M. Barrall. Evaluation of thermal transitions in some cholesteryl esters of saturated aliphatic acids. *Mol. Cryst. Liquid Cryst.* **10**:1–19 (1970).
26. J. H. Wendorff and F. P. Price. The structure of mesophases of cholesteryl esters. *Mol. Cryst. Liquid Cryst.* **24**:129–144 (1973).
27. K. Sakamoto, R.S. Porter, and J.F. Johnson. The viscosity of mesophases formed by cholesteryl myristate. In G. H. Brown (ed.), *Liquid Crystals 2,* Part II, Gordon and Breach Science Publishers, New York, 1969, pp. 237–249.
28. R. Finsy. Particle sizing by quasi-elastic light scattering. *Adv. Coll. Interface Sci.* **52**:79–143 (1994).
29. J. Snow and M. C. Philipps. Phase behavior of cholesteryl ester dispersions which model the inclusions of foam cells. *Biochemistry* **29**:2464–2471 (1990).
30. H. Bunjes, B. Siekmann, and K. Westesen. Emulsions of supercooled melts – a novel drug delivery system. In S. Benita (ed.), *Submicron Emulsions in Drug Targeting and Delivery*, Harwood academic publishers, Amsterdam, 1998, pp. 175–204.
31. M. J. Janiak, D. M. Small, and G. G. Shipley. Interactions of cholesterol esters with phospholipids: cholesteryl myristate and dimyristoyl lecithin. *J. Lipid Res.* **20**:183–199 (1979).
32. R. Van Antwerpen and J. C. Gilkey. Cryo-electron microscopy reveals human low density lipoprotein substructure. *J. Lipid Res.* **35**:2223–2231 (1994).